Size dependence of electron-phonon coupling in ZnO nanowires

R. P. Wang
Research Center for Advanced Photon Technology, Toyota Technological Institute 2-12-1, Hisakata, Tempaku-ku, Nagoya 468-8511, Japan

G. Xu and P. Jin
National Institute of Advanced Industrial Science and Technology (AIST), 2266-98 Anagahora, Shimoshidami, Moriyama-ku, Nagoya 463-8560, Japan

(Received 1 August 2003; revised manuscript received 20 November 2003; published 12 March 2004)

Raman spectra of ZnO powder and free-standing nanowires prepared by laser ablation have been studied. All observed vibrational modes in ZnO powder, both first order and higher order scattering, were assigned on the basis of group theoretical analysis. The size dependence of the coupling strength between electron and longitudinal optical (LO) phonon was experimentally estimated. It was found that the coupling strength determined by the ratio of second- to first-order Raman scattering cross sections diminishes with decreasing nanowire diameter, and the Frohlich interaction plays the main role in electron-phonon coupling in ZnO.

DOI: 10.1103/PhysRevB.69.113303 PACS number(s): 63.20.Kr, 78.30.Fs, 63.22.+m, 81.07.Vb

Coupling between electron and phonon is an important issue in semiconductor materials because it has significant influence on the optical and electrical properties of semiconductors, such as the energy relaxation rate of excited carriers and phonon replicas of excitons in the luminescence spectra. In a simple scenario, displacement of the partially ionic nuclei is accompanied by a radial electric field extending over many unit cells, and the potential of the displacement is proportional to the amplitude of the phonon. This electric field interacts Coulombically with the exciton, and the strength of such an exciton-phonon coupling will be enhanced if the wavelength of the phonon vibration is comparable to the spatial extent of the exciton.[1–9] So far, progress in material science has made it possible to prepare semiconductor nanocrystals that occupy volumes comparable with the size of the bulk exciton. Such quantum confined electronic systems should differ strongly from their bulk counterpart in their optical and electronic properties. Therefore a systematic study of the size dependence of the electron-phonon coupling strengths is of particular interest for understanding the fundamental physics and application to functional devices.

Theoretically, Schmitt-Rink, Miller, and Chemla suggested that the electron-LO-phonon coupling should vanish with decreasing size of the materials by using a simple charge neutrality model.[3] However, sophisticated theoretical treatments using the nonparabolicity of the bands showed an increasing coupling strength with decreasing nanocrystal size.[4,5] On the other hand, a series of experimental studies in CdSe, CdS, and InP nanocrystals indicated that the electron-phonon coupling diminishes with decreasing nanocrystal size,[2,6,7] while Klein and co-workers found that the electron-phonon coupling is size independent for CdSe.[8] Moreover, Scamarcio *et al.* reported an increase in the Frohlich-electron-LO-phonon interaction strength with decreasing size in CdS_xSe_{1-x} nanocrystals embedded in a glass slab.[9] Because of these contradictory results, the answer to this question is vague.

In this paper, we reported the measurement of the coupling between the lowest electronic excited state and LO modes in ZnO nanowires. ZnO has recently showed its great potential for applications in optical devices in the short wavelength region because of its wide band gap of 3.3 eV, and a highly efficient ultraviolet photoluminescence.[10–14] Much attention has been paid to the emission properties of ZnO, and room temperature ultraviolet lasing in ZnO has been demonstrated.[10–12] However, there are few attempts to study the electron-phonon coupling by Raman scattering experiments, which in principle can probe the electron-phonon coupling strength directly. On the other hand, the emission properties in ZnO have been found to be sensitive to the structural quality of the crystal though the origin and mechanism of many of the emission properties are still a matter of controversy. Moreover, the ZnO films were usually deposited on lattice-mismatched substrates such as sapphire and silicon, resulting in a large stress effect.[15] The stress would cause the shift of the phonon, and the difficulty in analyzing Raman scattering results. To circumvent this issue, we focused on free-standing ZnO nanowires synthesized by laser ablation of a pure Zn metal target. Raman spectrum was first taken on fine and commercially obtained ZnO powder. All observed vibrational modes, both first order and higher order scattering, were assigned on the basis of group theoretical analysis. Then Raman spectra were recorded on ZnO nanowires with different diameters. It was found that the electron-LO-phonon coupling strength, determined by the ratio of second- to first-order Raman scattering cross sections based on the well-built model,[2–9] decreases with decreasing nanowire diameter. These results will be helpful to understand the transport process and optical properties in ZnO materials.

The samples were prepared by the over-laser ablation method used for silicon nanowires as described in the experimental details of the synthesis in our previous work.[16] Briefly, a quartz tube was mounted inside a high-temperature tube furnace of 50 cm in length, and evacuated to a pressure of 1 Pa. High purity nitrogen was then passed through the quartz tube at a flow rate of 50 to 100 sccm. A fourth harmonic Nd:YAG laser (266nm) with a repetition rate of 5 Hz was used to ablate the target for 1 h while the temperature of

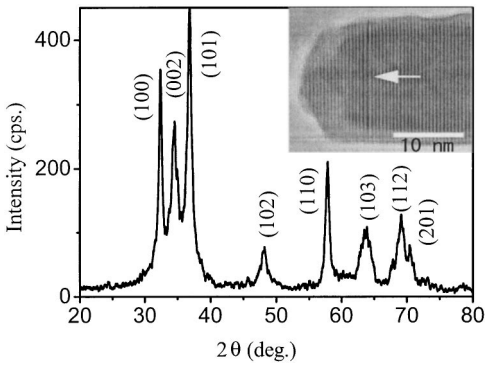

FIG. 1. X-ray diffraction pattern of ZnO nanowires. The inset is a high resolution TEM image of a tip of nanowire, and the arrow is marked along the growth direction.

the furnace was kept at 800 °C. The laser fluence was around 1.2 J/cm^2. The dark-gray product was collected from the wall of the quartz tube, and subsequently characterized by x-ray diffraction (XRD) and transmission electron microscopy (TEM). Only the peaks corresponding to wurtzite hexagonal structure of bulk ZnO could be found as shown in Fig. 1. The full width at half maximum of ZnO (002) peak is 0.52°. Transmission electron microscopy observation indicated that all nanowires grow along the (00*l*) direction with good crystallinity, and the average diameters change from 20 to 98 nm depending on the preparation conditions. The inset in Fig. 1 is a high resolution TEM image of a tip of the nanowires, from which the *c*-axis growth direction marked by the arrow is evident. We also checked the chemical composition of the as-grown samples by energy dispersive spectroscopy detector equipped in the TEM system. It was found that only Zn and O elements could be detected. Therefore we argue that, although ZnO nanowires are grown under nitrogen gas flow, the formation of ZnN_x is almost impossible due to its poor chemical stability at high growth temperature 800 °C. In contrast, the residual oxygen and probably also the leakage in our vacuum system assure the formation of ZnO. This argument is also supported by recent report, where Zhang *et al.* have successfully prepared ZnO nanowires under a constant flow of argon.[17]

Raman scattering experiments were performed at room temperature in a quasibackscattering geometry with parallel polarization incident light. A series of laser lines 266, 355, 488, and 514.5 nm were used as the excitation source. The incident light could be focused into a spot diameter of 10 μm and scan along the *x* or *y* direction. The scattered light from the sample was passed through a broadband polarization scrambler to eliminate polarization effects in the monochromator. Under this optical geometry, Raman spectra is insensitive to the random orientation of respective nanowires since all unpolarized scattered light can be collected. The laser power was kept at 0.2 mW. The spectra were recorded by using a 16-bit charge coupled device detector. For each exciting wavelength, we measured several different positions in order to achieve the maximum enhancement of the first Raman scattering peaks. Special care has been taken to keep the same measurement conditions for different excitation wavelength.

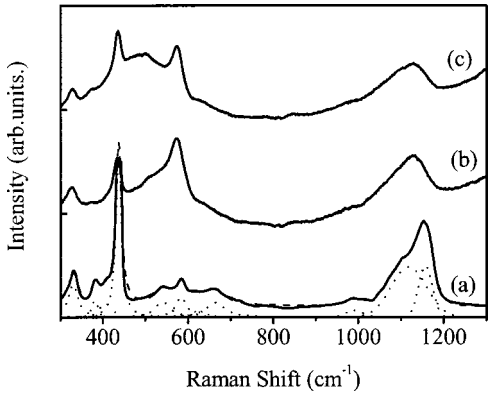

FIG. 2. Raman spectra of ZnO powder and nanowires excited by 355 nm incident laser. (a) The solid line is the experimental result for ZnO powder, the dashed line is fitting of the whole spectrum, and the dotted lines are fitting of the separated peaks. (b) ZnO nanowires with the diameter of 44 nm. (c) ZnO nanowires with the diameter of 20 nm. All spectra were excited by 355 nm laser line with the power of 0.2 mW. Both (b) and (c) are multiplied by 6 and shifted upward in the same units for clarity. The baseline for (b) and (c) is also marked.

Raman spectrum of the fine ZnO powder was shown in Fig. 2.(a), where the peaks at 331, 383, 438, 549, 584, and 660 cm^{-1} were clearly observed in the low wave-number region. Moreover, there is a very weak shoulder located at the low energy side of 438 cm^{-1} peak, which corresponds to the E_1(TO) at 410 cm^{-1}. On the other hand, several peaks located, respectively, at 987, 1101, and 1154 cm^{-1} were also found at the large wave-number region from 700 to 1300 cm^{-1}. No more high-order peaks could be observed at the region over 1300 cm^{-1}. We have deconvoluted Raman spectrum into a series of separated peaks as shown Fig. 2(a) by the nonlinear least-squares optimization method. All peaks were assigned on the basis of group theoretical analysis. The results as well as a comparison with the previous works were listed at Table I, from which a good agreement is evident.

Typical Raman spectra of ZnO nanowires with diameters

TABLE I. Wave number (in cm^{-1}) and symmetries of the modes found in Raman spectrum of hexagonal ZnO powder and their assignments.

Wave number	Symmetry	Process	Ref. 18	Ref. 21
331	A_1	Acoust. Overtone		
383	A_1(TO)	First process	381	397
410	E_1(TO)	First process	407	426
438	E_2	First process	441	449
540	A_1(LO)	First process		559
584	E_1(LO)	First process	583	577
660	A_1	Acoust. Overtone		
776	A_1, E_2	Acoust. Opt. comb.		
987	A_1, E_2	Opt. Comb.		
1101	A_1, E_2	Acoust. comb.		
1154	A_1	Opt. overtone		

of 44 and 20 nm were shown in Figs. 2(b) and 2(c), respectively. Compared with its bulk counterpart, several obvious changes could be observed. First, in the low wave-number region only the 331, 438, and 584 cm^{-1} peaks persist well when the diameter decreases to nanometer scale, while the 383 and 540 cm^{-1} peaks become very weak and broad. In addition, 987 and 1101 cm^{-1} peaks at large wave-number region seems to hide themselves behind the broad background, leading to an asymmetrical and board 1154 cm^{-1} peak. Furthermore, the intensities of all observed vibrational modes decrease and their lineshapes become asymmetric, and some observed modes shift to lower wave number with decreasing nanowire diameters compared with Fig. 2(a).

It is well known that phonon eigenstates in an ideal crystal are plane waves due to the infinite correlation length; therefore the $K=0$ momentum selection rule of the first order Raman spectrum can be satisfied. When the crystalline is reduced to nanometer scale, the momentum selection rule will be relaxed. This allows the phonon with the wave vector $|k|=|k'|\pm 2\pi/L$ to participate in the first-order Raman scattering, where k' is the wave vector of the incident light and L is the size of the crystal. The phonon scattering will not be limited to the center of the Brillouin zone, and the phonon dispersion near the zone center must also be considered. As a result, the shift, broadening, and the asymmetry of the first order optical phonon can be observed. In the present experiments, because of the random alignment of nanowires, Raman scattering measurements under such optical geometry in this study, in principle, should detect all Raman active modes as shown in Fig. 2(a) for ZnO powder. However, an intrinsic problem for oxide material is oxygen deficient in the growth process of nanowires. For ZnO bulk material with the wurtzite structure where close-packed layers of Zn and oxygen are stacked alternately along the c axis, the lattice irregularity such as oxygen defects along the c axis would more directly affect the displacement of ions in the A_1 modes (along the c axis) than in the E_1(TO) modes (in a-b plane), which leads to a quick decrease in the intensity of A_1 modes.[15] To further check this point, we also measured Raman spectrum of ZnO nanowires annealed at 600 °C and under oxygen flow for 2 h. The weak A_1 mode could be found, but the ratio of second- to first-order Raman scattering cross section of E_1(LO) modes is almost insensitive to heating process. Moreover, we also rotated the sample with 90° and measured Raman spectrum at the same position, no observable shift of Raman peaks confirms that the random orientation of nanowires have negligible effect on the results in this study. On the other hand, we had already pointed out some possible effects leading to the shift, broadening, and the asymmetry of the first order optical phonon in silicon nanowires in our previous study, we found that phonon confinement plays a main role in determining these changes.[16] The same conclusion can be applied to ZnO nanowires, in which the direction of phonon shift is determined by the phonon dispersion curve. A detailed study on this issue will be reported separately.

Of special interest in this study is to extract information of the electron-phonon coupling from Raman scattering data, which had never been reported for ZnO materials before. Previously, people have intensely studied CdS, CdSe, and InP nanoparticles by this method.[2–9] The ratio between second- and first-order scattering cross section was found to be a very sensitive function of the electron-phonon coupling strength[8,9]

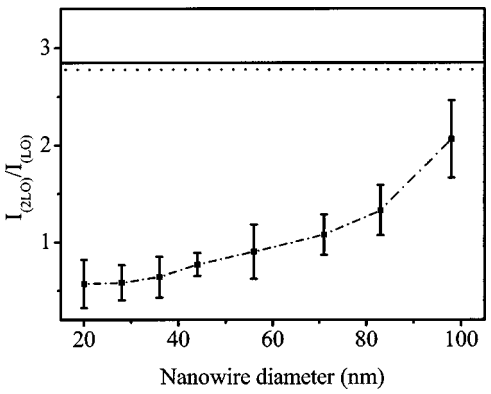

FIG. 3. Ratio between second- and first-order Raman scattering cross section as a function of the diameter of nanowire. The solid and dotted lines are, respectively, corresponding to the ratio calculated from Eq. (1) and experimentally obtained for ZnO powder. The dashed line joining the points is a guide for the eye.

$$\Delta^2=\frac{e^2}{a}\left(\frac{24}{\pi}\right)^{1/3}\frac{1}{\hbar\omega_{\mathrm{LO}}}\left(\frac{1}{\varepsilon_\infty}-\frac{1}{\varepsilon_0}\right)\frac{1}{w}\int_0^w\frac{x^4(2+x^2)^2}{(1+x^2)^4}dx, \tag{1}$$

where $w=(3\pi^2)^{1/2}a_0/a$ and a_0, a are the exciton radius and lattice parameter, respectively. Δ is known to be related to the Huang-Rhys parameter S by the relation $S=\Delta^2$. For bulk ZnO materials, Δ is calculated to be 2.85 based on Eq. (1), which is in an excellent agreement with the experimental value 2.78, the ratio of second- to first-order scattering cross section for ZnO powder from Fig. 2(a). We have measured a series of nanowire samples and deconvoluted Raman spectra into separated peaks. The ratio as a function of the diameter of nanowire was plotted in Fig. 3. The value of the ratio was found to increase with increasing nanowire diameter. Those calculated from Eq. (1) and experimentally obtained for ZnO powder were also indicated in Fig. 3 for reference. We should emphasize that it is not meaningful to compare the electron-phonon coupling strength in nanowire with its bulk counterpart. For bulk materials, all scattering process should follow the momentum conservation conditions, while this rule is relaxed for nanocrystal. Furthermore, the quantum confinement strongly modifies the eigenfunctions in nanometer scale materials, and causes the change of the exciton radius and dielectric coefficient and finally has profound consequences on the magnitude of the coupling.

Callender *et al.*[8] have studied the resonant Raman scattering in ZnO bulk crystal. They measured the dispersion of the Raman scattering cross section of several phonon modes using a wide range of laser energies, and found that all TO modes in ZnO crystal are almost dispersionless while the intensity of E_1(LO) is greatly enhanced under the resonant conditions. For example, they found that the ratio of second- to first-order E_1(LO) scattering cross section changes from 2 by using 350.7 nm incident laser line to 24 by using 356.4

nm line for ZnO crystal. In our Raman scattering experiments, although some phonons hide behind the broad background around E_1(LO) and its overtone, our deconvolution process can resolve this issue well. The ratio of second- to first-order scattering cross section 2.78 for ZnO powder by using 355 nm incident laser line in our study, is reasonably comparable to Callender *et al.* results, confirming that uncertainty caused by the deconvolution process is too small to affect our conclusion.

Scamarico *et al.* recently argued that keeping constant the resonance condition is mandatory for a meaningful comparison of spectra associated with nanocrystal having different sizes and hence different electron transitions due to the strong energy dependence of the Raman scattering cross section.[9] In this study, we have carefully used the same experimental conditions such as laser power, spot size, and so on for each sample. Although our smallest sample is still larger than the exciton radius of ZnO bulk material, we reported here with an emphasis on the *tendency* of the decreasing electron-phonon interaction with decreasing nanocrystal size. So far there is no reported way to prepare ZnO nanowire with the size smaller than the exciton radius, therefore the exact behavior of electron phonon coupling in very small scale is still a research target in the future. Our results are also supported by Makino and co-workers who, using the absorption and photoluminescence spectra, found that the Huang-Rhys parameter S in $ZnO/Mg_{0.27}Zn_{0.73}O$ quantum wells, which determines the strength of the electron-phonon interaction, increases significantly when the well width increases.[13–14]

Let us move to the origin of electron-phonon coupling in ZnO nanowires. It is generally accepted that the electron phonon coupling is governed by two mechanisms: the deformation potential and the Frohlich potential. Following Loudon[19] and Kaminow and Johnston,[20] the TO Raman scattering cross section is mainly determined by the deformation potential that involves the short-range interaction between the lattice displacement and the electrons. On the other hand, the LO Raman scattering cross section includes contributions from both the Frohlich potential that involves the long-range interaction generated by the macroscopic electric field associated with the LO phonons and the deformation potential. We found that the intensity of TO phonon in ZnO nanowire is almost insensitive to the incident laser wavelength, while that of E_1(LO) phonon is greatly enhanced under the resonant conditions. Therefore we believe that the electron-LO interaction at decreasing the nanocrystal size is mainly associated with the Frohlich interaction.

In summary, we have measured Raman spectra of ZnO powder and nanowires with different diameters. Based on the group theoretical analysis, we have assigned all observed vibrational modes. The shift, broadening, and the asymmetry of the optical phonons have been found for ZnO nanowires compared with their bulk counterpart. The phonon confinement effect could account for these observed results. Moreover, we have extracted the electron-phonon-coupling parameter from Raman spectra, and unambiguously demonstrate that electron-phonon-coupling increase with increasing nanocrystal size mainly due to the Frohlich interaction.

[1] The relevant exciton-phonon coupling mechanisms in the bulk have been extensively discussed by A. Pinczuk and E. Burstein, in *Light Scattering in Solid I*, edited by M. Cardona (Springer, Berlin, 1983).

[2] A.P. Alivisatos, T.D. Harris, P.J. Carroll, M.L. Steigerwald, and L.E. Brus, J. Chem. Phys. **90**, 3463 (1989).

[3] S. Schmitt-Rink, D.A.B. Miller, and D.S. Chemla, Phys. Rev. B **35**, 8113 (1987).

[4] J.C. Marini, B. Stebe, and E. Kartheuser, Phys. Rev. B **50**, 14 302 (1994).

[5] S. Nomura and T. Kobayashi, Phys. Rev. B **45**, 1305 (1992).

[6] J.J. Shiang, S.H. Risbud, and A.P. Alivisatos, J. Chem. Phys. **98**, 8432 (1993).

[7] J.J. Shiang, R.H. Wolters, and J.R. Heath, J. Chem. Phys. **106**, 8981 (1997).

[8] M.C. Klein, F. Hache, D. Ricard, and C. Flyzanis, Phys. Rev. B **42**, 11 123 (1990).

[9] G. Scamarcio, V. Spagnolo, G. Ventruti, M. Lugara, and G.C. Righini, Phys. Rev. B **53**, R10 489 (1996).

[10] S. Cho, J. Ma, Y. Kim, Y. Sun, G.K.L. Wong, and J.B. Ketterson, Appl. Phys. Lett. **75**, 2761 (1999).

[11] M.H. Huang, S. Mao, H. Feick, H. Yan, Y. Wu, H. Kind, E. Weber, R. Russo, and P. Yang, Science **292**, 1897 (2001).

[12] H. Cao, Y.G. Zhao, H.C. Ong, S.T. Ho, J.Y. Dai, J.Y. Wu, and R.P.H. Chang, Appl. Phys. Lett. **73**, 656 (1998).

[13] T. Makino, K. Tamura, C.H. Chia, Y. Segawa, M. Kawasaki, A. Ohtomo, and H. Koinuma, Phys. Rev. B **66**, 233305 (2002).

[14] H.D. Sun, T. Makino, N.T. Tuan, Y. Segawa, M. Kawasaki, A. Ohtomo, K. Tamura, and H. Koinuma, Appl. Phys. Lett. **78**, 2464 (2001).

[15] M. Gomi, N. Oohira, K. Ozaki, and M. Koyano, Jpn. J. Appl. Phys. **42**, 481 (2003).

[16] R.P. Wang, G.W. Zhou, Y.L. Liu, S.H. Pan, H.Z. Zhang, D.P. Yu, and Z. Zhang, Phys. Rev. B **61**, 16 827 (2000).

[17] Y. Zhang, H. Jia, X. Luo, X. Chen, D. Yu, and R. Wang, J. Phys. Chem. B **107**, 8289 (2003).

[18] R.H. Callender, S.S. Sussman, M. Selders, and R.K. Chang, Phys. Rev. B **7**, 3788 (1973).

[19] R. Loudon, Adv. Phys. **13**, 23 (1964).

[20] I.P. Kaminow and W.D. Johnston, Phys. Rev. **160**, 19 (1967).

[21] F. Decremps, J.P. Porres, A.M. Saitta, J.C. Chervin, and A. Polian, Phys. Rev. B **65**, 092101 (2002).